Sandia National Laboratories

Exceptional service in the national interest

ME469: Multiphase Methods:
Volume of Fluid Methods

Stefan P. Domino[1,2]

[1] Computational Thermal and Fluid Mechanics, Sandia National Laboratories

[2] Institute for Computational and Mathematical Engineering, Stanford

This presentation has been authored by an employee of National Technology & Engineering Solutions of Sandia, LLC under Contract No. DE-NA0003525 with the U.S. Department of Energy (DOE). The employee owns all right, title and interest in and to the presentation and is solely responsible for its contents. The United States Government retains and the publisher, by accepting the article for publication, acknowledges that the United States Government retains a non-exclusive, paid-up, irrevocable, world-wide license to publish or reproduce the published form of this article or allow others to do so, for United States Government purposes. The DOE will provide public access to these results of federally sponsored research in accordance with the DOE Public Access Plan https://www.energy.gov/downloads/doe-public-access-plan.

SAND2018-4536 PE

U.S. DEPARTMENT OF ENERGY

NNSA

Objective: Model Multiphase Flow (Air/Water)

Validation case of Kleefsman et al. *"A volume-of-fluid based simulation method for wave impact problems"*, J. Comput. Phys. (2005).

See:

/laboratory/3d_hex8_dam_break

(nuances associated with top and bottom simulation will be captured later in the lecture)

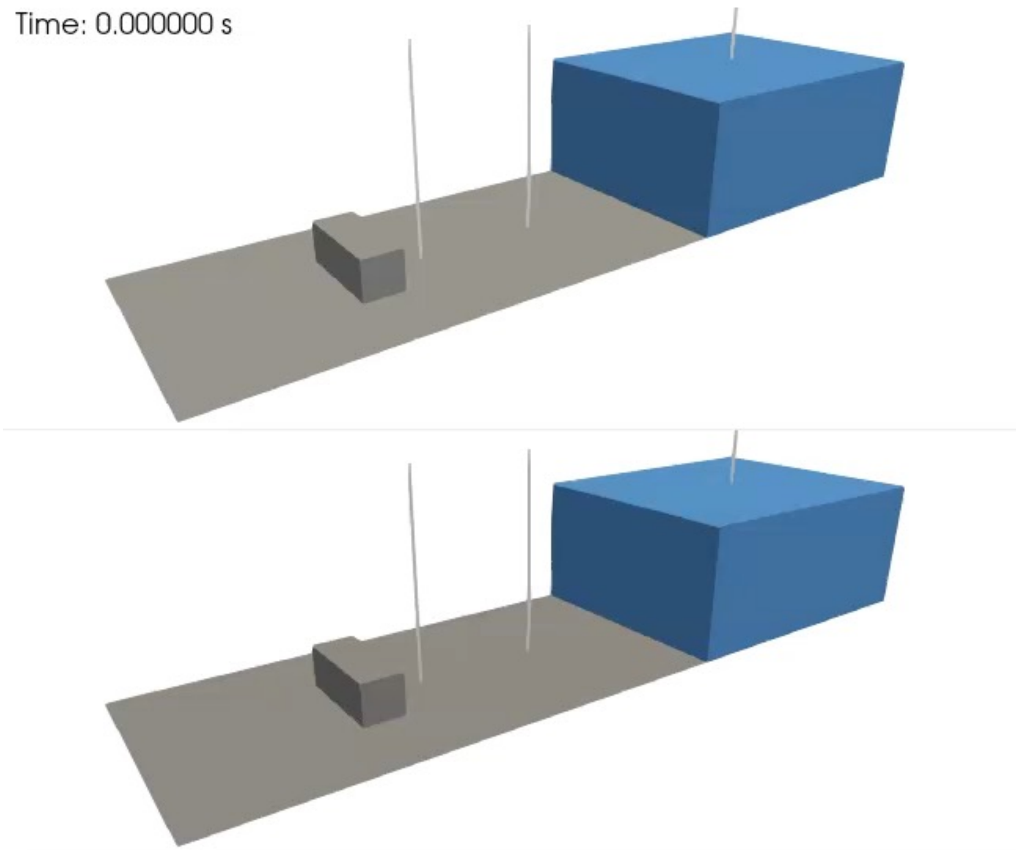

Goals:

- What multiphase method: Volume of Fluid (VOF) or level set? (sometimes VoF)
- Consistency established via a “balanced force scheme”
- Verification for VOF equation
  - Using routine and improved advection operators
- Surface sharpening
- Capillary instability
- All together for general air/liquid modeling and simulation
  - Validation

Step 1: Definition of an Air/Liquid Interface (Phase 1/Phase 2)

Signed-distance function (level-set), Ψ

- Popularized by Osher and Sethian, "Fronts propagating with curvature-dependent speed: Algorithms based on Hamilton-Jacobi formulations", J. Comp. Phys., 1988,

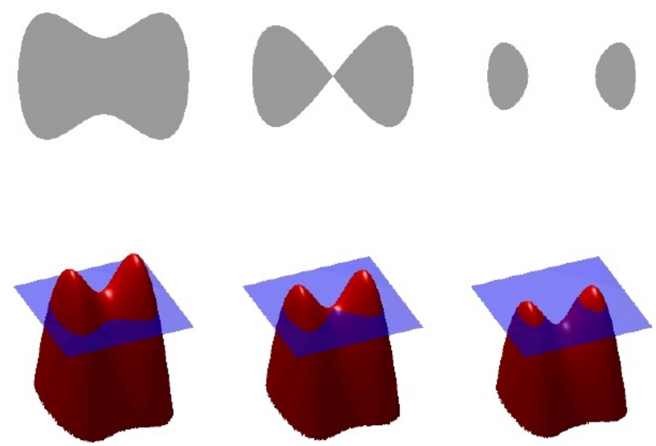

Ψ defines an zero-isocontour, with distance (+/- in either direction)

Volume of Fluid, ϕ or α

- Lineage classically provided to *Noh, W.F.; Woodward, P. (1976). van de Vooren, A.I.; Zandbergen, P.J. (eds.). SLIC (Simple Line Interface Calculation). proceedings of 5th International Conference of Fluid Dynamics. Lecture Notes in Physics. Vol. 59. pp. 330–340*
- Interpretation: volume fraction of phase 1, interphase lives at ½

$$\rho = \alpha\rho^{\alpha=1} + (1-\alpha)\rho^{\alpha=0} \qquad \frac{\partial \alpha}{\partial t} + u_j \frac{\partial \alpha}{\partial x_j} = 0$$

$$n_j^I = \frac{\frac{\partial \alpha}{\partial x_j}}{\left|\frac{\partial \alpha}{\partial x_j}\right|} \qquad \kappa = -\frac{\partial n_j^I}{\partial x_j}$$

Interface normal and curvature

Step 1: Definition of an Air/Liquid Interface (Phase 1/Phase 2)

Signed-distance function (level-set), Ψ

- Popularized by Osher and Sethian, "Fronts propagating with curvature-dependent speed: Algorithms based on Hamilton-Jacobi formulations", J. Comp. Phys. (1988)

Volume of Fluid, ϕ or α

- Lineage classically provided to *Noh, W.F.; Woodward, P. (1976). van de Vooren, A.I.; Zandbergen, P.J. (eds.). SLIC (Simple Line Interface Calculation). proceedings of 5th International Conference of Fluid Dynamics. Lecture Notes in Physics. Vol. 59. pp. 330–340*
- Interpretation: volume fraction of phase 1, interphase lives at ½

$$\rho = \alpha\rho^{\alpha=1} + (1-\alpha)\rho^{\alpha=0} \qquad \frac{\partial \alpha}{\partial t} + u_j \frac{\partial \alpha}{\partial x_j} = 0$$

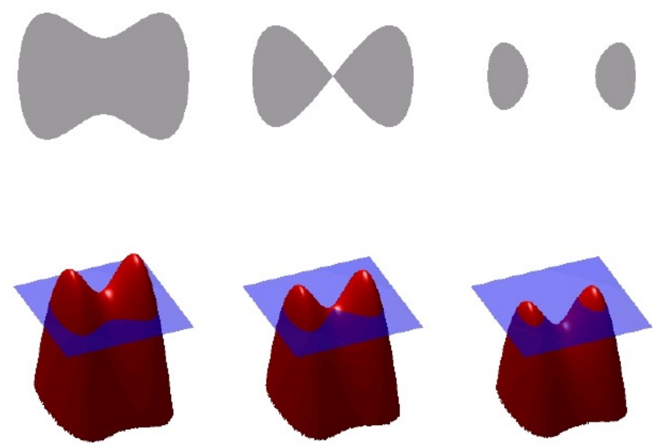

Ψ defines an zero-isocontour, with distance (+/- in either direction)

$$n_j^I = \frac{\frac{\partial \alpha}{\partial x_j}}{|\frac{\partial \alpha}{\partial x_j}|} \qquad \kappa = -\frac{\partial n_j^I}{\partial x_j}$$

Interface normal and curvature

VOF Transport Discretization Nuance: Volume- or Surface-based?

- Simple enough, define the volume (fraction) of fluid (absent evaporation): $\frac{\partial \alpha}{\partial t} + u_j \frac{\partial \alpha}{\partial x_j} = 0$

Option 1: volumetric-form: $\int \frac{\partial \alpha}{\partial t} dV + \int u_j \frac{\partial \alpha}{\partial x_j} dV = 0$

CVFEM/FEM (really, any element-based approach)
Evaluated as a volumetric-contribution (diamonds)

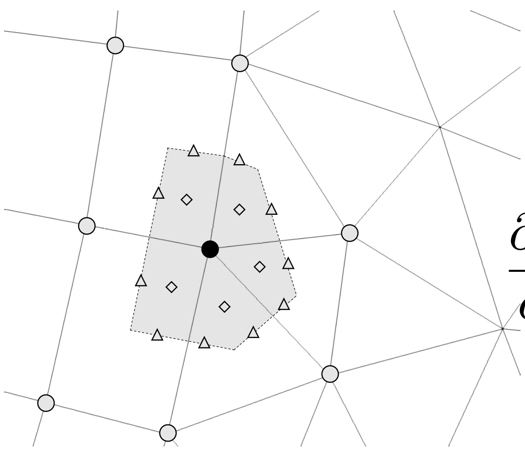

$$\phi_{ip} = \sum_n N_n^{ip} \phi_n$$

$$\frac{\partial \phi_{ip}}{\partial x_j} = \sum_n \frac{\partial N_n^{ip}}{\partial x_j} \phi_n$$

Option 2: divergence-form:

$$\int \frac{\partial \alpha}{\partial t} dV + \int \frac{\partial \alpha u_j}{\partial x_j} dV - \int \alpha \frac{\partial u_j}{\partial x_j} dV = 0$$

Gauss-Divergence $\int \alpha \hat{u}_j n_j dS$

Traditional finite volume (element, edge, cell-centered)
Evaluated as a surface integral (triangle)

Allows for a consistent advecting velocity (mass conserving) that is obtained from the continuity equation

Equal-Order Interpolation, i.e., Collocation:
Q: If F_i includes surface tension, however, $\hat{u}_j$ does not, then what?

- Lack of consistency between continuity and momentum system leads to parasitic currents – even for a static bubble arrangement
  - Goal: static equilibrium where surface tension balances pressure gradient perfectly

$$\int \left(\frac{\partial \rho^{k+1} u_i^{k+1}}{\partial t} + G_i p^k \right) dV + \int \rho^{k+1} \hat{u}_j u_i^{k+1} n_j dS = \int 2\mu S_{ij}^{*k+1} n_j dS + \int F_i dV$$

$$\int \frac{\partial \rho^{k+1}}{\partial t} dV + \int \rho^{k+1} \hat{u}_j n_j dS = 0$$

$$\hat{u}_j = u_j - \frac{\tau}{\rho} \left(\frac{\partial p}{\partial x_j} - G_j p \right)$$

$$F_i = \sigma \kappa \frac{\partial \alpha}{\partial x_i} \quad n_j^I = \frac{\frac{\partial \alpha}{\partial x_j}}{\left| \frac{\partial \alpha}{\partial x_j} \right|} \quad \kappa = -\frac{\partial n_j^I}{\partial x_j}$$

σ and κ are surface tension and curvature (recall, interface normal), see: Brackbill et al. "A continuum method for modeling surface tension", J. Comp. Phys. (1992)

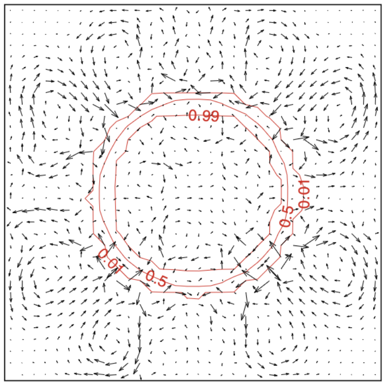

Harvie et al. "An analysis of parasitic current generation in Volume of Fluid simulations", App. Math. Modeling (2006)

Equal-Order Interpolation, i.e., Collocation: Pressure Stabilization Review

- $\hat{u}_j$ is a function of the fine-scale momentum residual (evaluated at an integration point):

$$\hat{u}_j = u_j - \frac{\tau}{\rho} R^h(u_j) \qquad R^h(u_j) = \frac{\partial \rho u_i}{\partial t} + \frac{\partial \rho u_j u_i}{\partial x_j} - \frac{\partial}{\partial x_j} 2\mu S^*_{ij} + \frac{\partial p}{\partial x_i} - F_i \quad (1)$$

We can also project this residual to the nodes, $\hat{R}^h(u_j) = T_i + A_i - D_i + G_i - F_i$ and approximate $R^h(u_j)$ as re-interpolation of choice terms

- Usage of a full residual (1) results in a classic Pressure Stabilized Petrov Galerkin (Hughes et al. 1986)
- Pick and choose each residual, Majumdar (1988)
- Algebraically manipulation affords the classic Rhie-Chow-based (1983) pressure stabilization

$$\hat{u}_j = u_j - \frac{\tau}{\rho}\left(\frac{\partial p}{\partial x_j} - G_j p\right) \qquad \textbf{~ (L-DG)}$$

  - shown to be stable and dissipative [Ham and Iaccarino (2004) or Domino (2006)]
- There is also the nuance of pressure projection vs monolithic

VOF using Balanced Force: Brief Survey

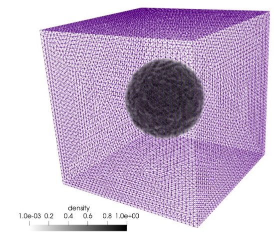

Static bubble $\rho \rightarrow 1000{:}1$

- Classic Balanced Force, Francois, J. Comput. Phys. (2006)
- First CVFEM: Lin et al, J. Comput. Phys. (2019)
- Parasitic currents suppressed via a consistent momentum/continuity stabilization form: fine-scale momentum residual algebraically modified in continuity equation

$$\int \left(\frac{\partial}{\partial t} \rho^* u_i^{k+1} + \rho^* \hat{G}_i p^k \right) \mathrm{d}V + \int \rho^* \hat{u}_j u_i^{k+1} n_j \mathrm{d}S$$
$$= \int \mu^* \left(\frac{\partial u_i^{k+1}}{\partial x_j} + \frac{\partial u_j^{k+1}}{\partial x_i} \right) n_j \mathrm{d}S + \int \gamma \rho^* g_i \mathrm{d}V$$

Momentum Equation

$$\hat{G}_\beta p^k = \frac{\sum_{ip} \frac{1}{\rho^*} \left(\frac{\partial p^k}{\partial x_\beta} - \sigma \kappa \frac{\partial \alpha}{\partial x_\beta} - \gamma \rho^* g_\beta \right) |A_\beta|}{\sum_{ip} |A_\beta|}$$

Nodal pressure gradient

$$-\int \frac{1}{\rho^*} \frac{\partial \Delta p^{k+1}}{\partial x_j} n_j \mathrm{d}S = -\frac{1}{\Delta t} \int \hat{u}_j n_j \mathrm{d}S$$

Continuity Equation

$$\hat{u}_j = u_j^{R,k} - \Delta t \left(\frac{1}{\rho^*} \left(\frac{\partial p^k}{\partial x_j} - \sigma \kappa \frac{\partial \alpha}{\partial x_j} - \gamma \rho^* g_j \right) - \hat{G}_j p^k \right)$$

Convecting-velocity

Note: benefits from ρg_i ($\gamma = 1$) included in stabilization

VOF using Balanced Force: Brief Survey

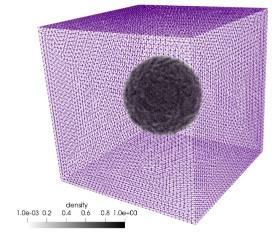

Static bubble $\rho \rightarrow 1000:1$

- Classic Balanced Force, Francois, J. Comput. Phys. (2006)
- First CVFEM: Lin et al, J. Comput. Phys. (2019)
- Parasitic currents suppressed via a consistent momentum/continuity stabilization form: fine-scale momentum residual algebraically modified in continuity equation

$$\int \left(\frac{\partial}{\partial t}\rho^* u_i^{k+1} + \rho^* \hat{G}_i p^k\right) \mathrm{d}V + \int \rho^* \hat{u}_j u_i^{k+1} n_j \mathrm{d}S = \int \mu^* \left(\frac{\partial u_i^{k+1}}{\partial x_j} + \frac{\partial u_j^{k+1}}{\partial x_i}\right) n_j \mathrm{d}S + \int \gamma \rho^* g_i \mathrm{d}V$$

Momentum Equation

$$-\int \frac{1}{\rho^*} \frac{\partial \Delta p^{k+1}}{\partial x_j} n_j \mathrm{d}S = -\frac{1}{\Delta t} \int \hat{u}_j n_j \mathrm{d}S$$

Continuity Equation

$$\hat{G}_\beta p^k = \frac{\sum_{ip} \frac{1}{\rho^*}\left(\frac{\partial p^k}{\partial x_\beta} - \sigma\kappa \frac{\partial \alpha}{\partial x_\beta} - \gamma \rho^* g_\beta\right) |A_\beta|}{\sum_{ip} |A_\beta|}$$

Surface tension Continuum Surface Force (CSF)

$$\hat{u}_j = u_j^{R,k} - \Delta t \left(\frac{1}{\rho^*}\left(\frac{\partial p^k}{\partial x_j} - \sigma\kappa \frac{\partial \alpha}{\partial x_j} - \gamma \rho^* g_j\right) - \hat{G}_j p^k\right)$$

Note: benefits from ρg_i ($\gamma = 1$) included in stabilization

Common "Verification test"

- Static bubble (image shown for the density ratio 1000:1)

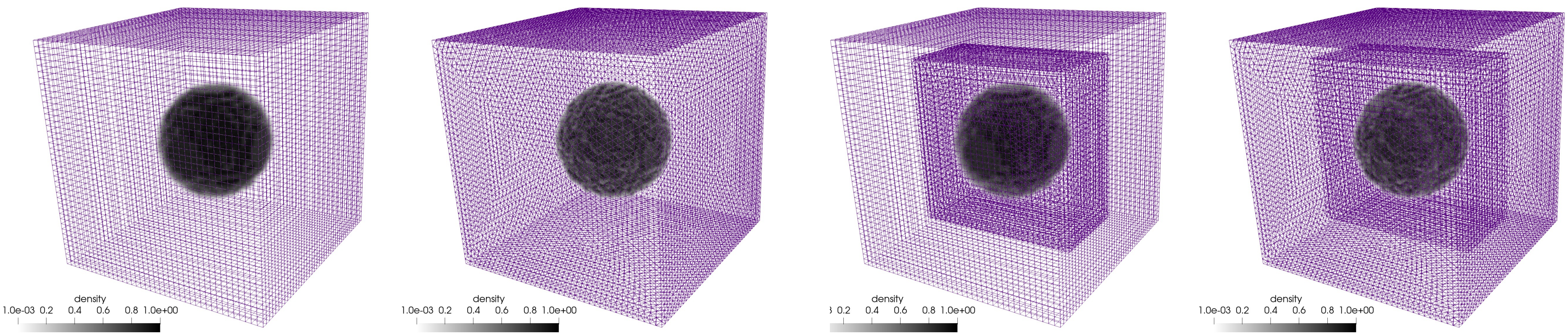

Hex8, Tet4, Hex8/Tet4, Tet4./Hex8

Table A.2

Errors in velocity after one time step for the viscous static bubble case exercising both the conformal and overset mesh configuration.

$\frac{\rho_1}{\rho_2}$	Hex8	Tet4	Hex8/Tet4	Tet4/Hex8
10	9.8796e−05	0.000399404	0.000282716	0.000362421
100	0.000118674	0.000725406	0.000319116	0.000627669
1000	0.000121508	0.000795518	0.000323546	0.000730521

Simple Verification Test for: $\dfrac{\partial \alpha}{\partial t} + u_j \dfrac{\partial \alpha}{\partial x_j} = 0$

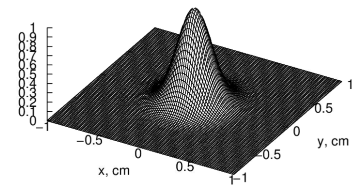

- Molenkamp verification, see Martinez, Int. J. Numer. Meth. Engr. (2004), shown below with a variety of stabilization options

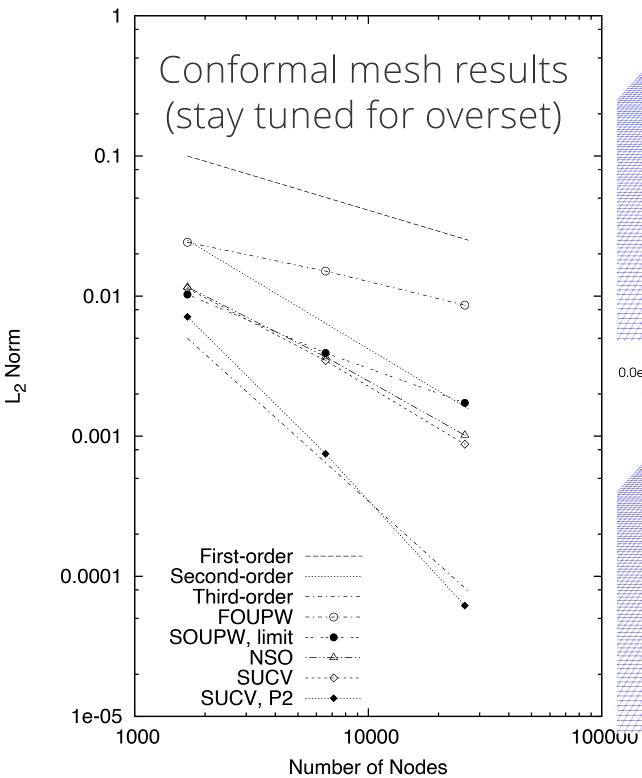

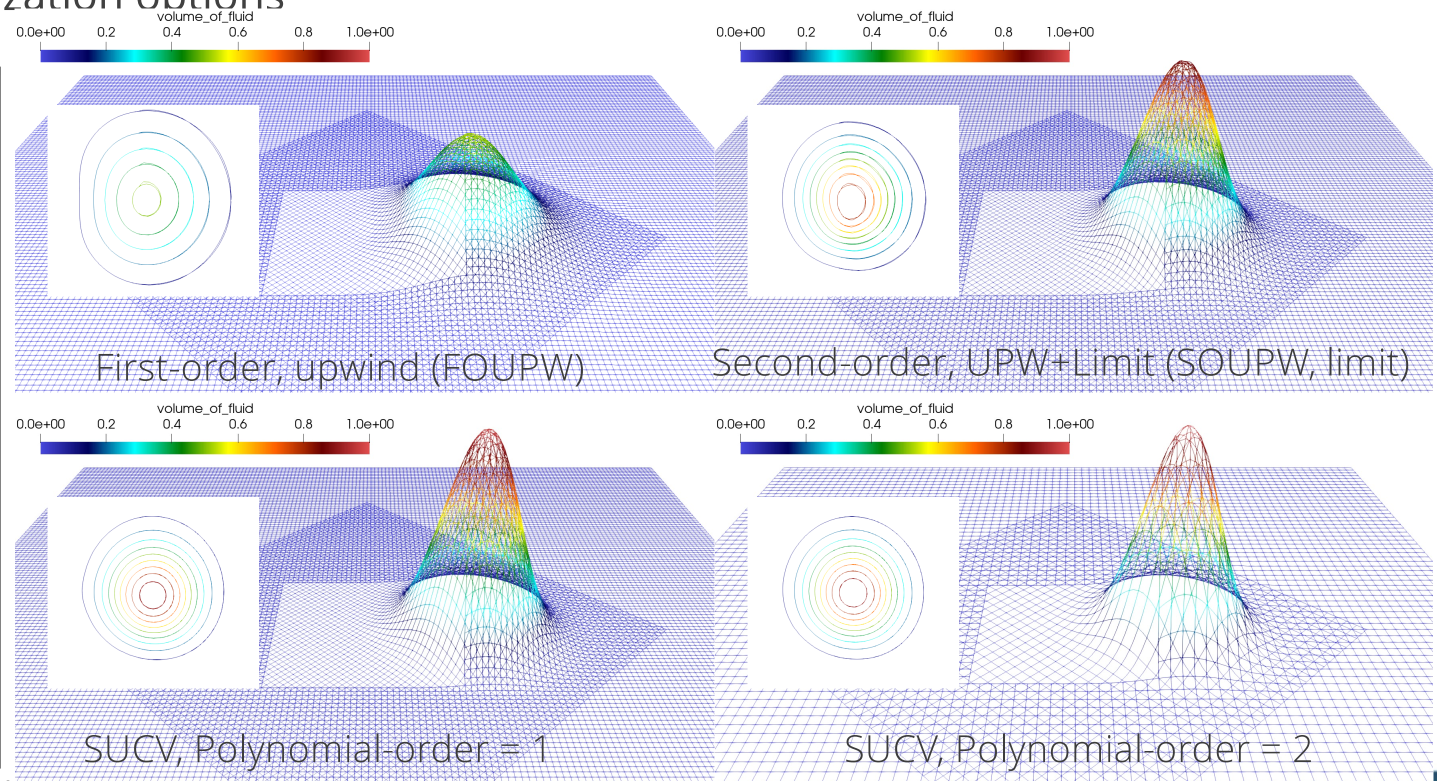

Passive Transport Example: Driven Cavity

- Exploring PDE-based sharpening, interface smoothing and stabilization

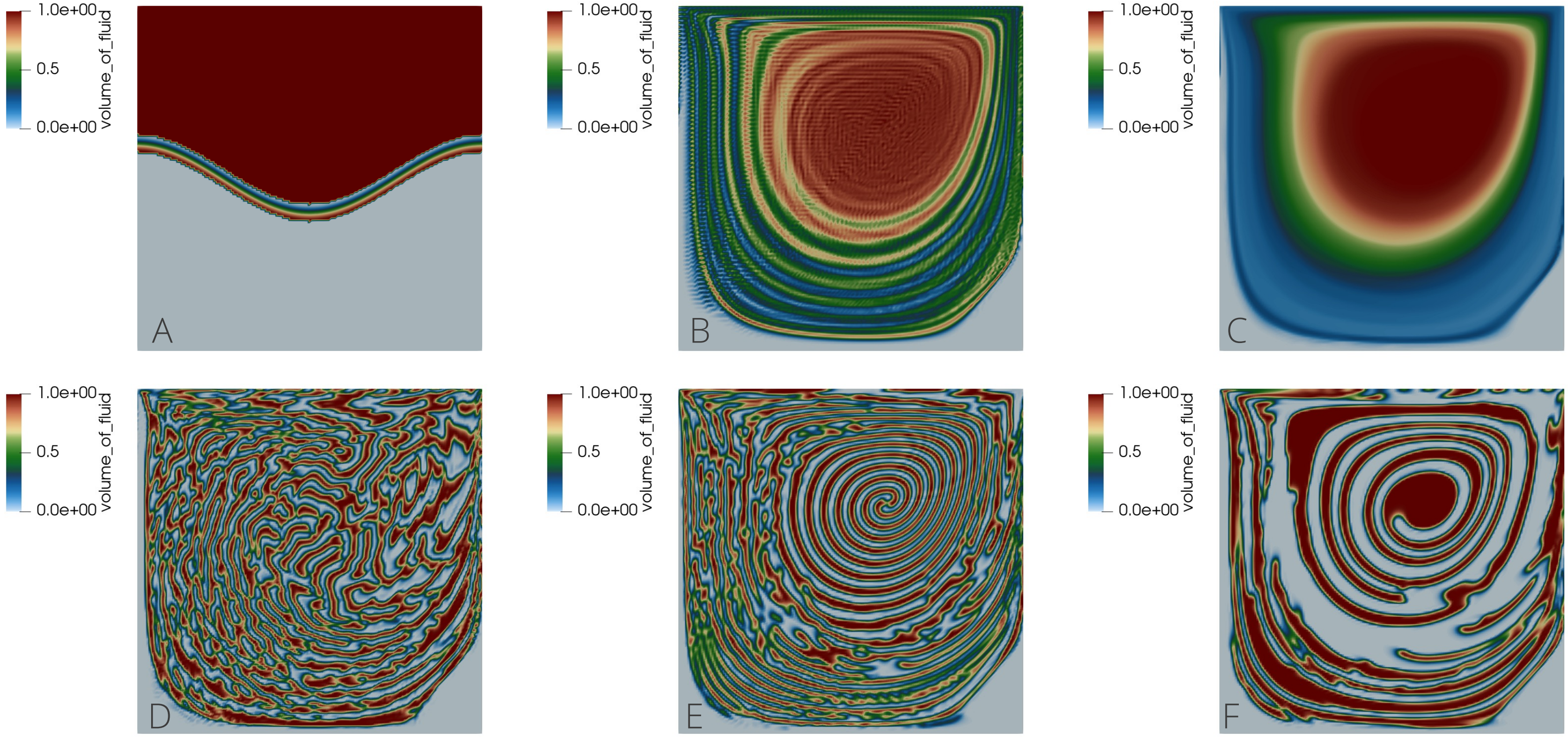

A. Initial condition
B. No stabilization
C. SUCV+NSO
D. Sharpening+B
E. Sharpen+C
F. E+Smoothing

VOF Transport: Sharpening + Advection Stabilization + Interface Smoothing

VOF equation with PDE-based sharpening (to mitigate numerical diffusion) that includes residual-based stabilization

$$\int \frac{\partial \alpha}{\partial t}\mathrm{d}V + \int \alpha \hat{u}_j n_j \mathrm{d}S$$

Integrated-by-parts advection to allow for consistent continuity constraint; $R^h(\alpha)$

$$- \int \frac{\partial s_j}{\partial x_j}\mathrm{d}V$$

PDE-based sharpening with compression velocity in the direction of the interface normal, n_j^I

$$s_j = -u_{c_j}\alpha\,(1-\alpha)$$

$$u_{c_j} = C_\alpha |u_k - v_k| n_j^I$$

$$- \sum_e \int \tau^h u_j^R R^h(\alpha) n_j \mathrm{d}S$$

Streamwise-upwind, control volume (SUCV), Swaminanthan et al., Int. J. Numer. Meth. Engr. (1993); based on Streamwise Upwind Petrov-Galerkin (SUPG), Brooks and Hughes, Comput. Methods in Appl. Mech. Eng. (1982).

$$- \sum_e \int \nu^h g^{ij} \frac{\partial \alpha}{\partial x_j} n_i \mathrm{d}S = 0$$

Nonlinear stabilization operator (NSO); Motivated by Shakib et. al, Comput. Methods in Appl. Mech. Eng. (1991), discontinuity capturing operator (later termed NSO); $\nu^h = f(R^h(\alpha))$ NSO and SUCV avoids common gradient reconstruction techniques commonly used in unstructured formulations, see Tsui et al., Int. J. Heat Mass Trans. (2009)

$$n_j^I = \frac{\sum_{scv} \left(\frac{\partial \alpha}{\partial x_j}\right)_{scv} V_{scv}}{\left(||\frac{\partial \alpha}{\partial x_j}||_{scv} + \epsilon\right) \sum_{scv} V_{scv}}$$

Nuance: interface normal can be computed using a smoothed VOF field

Alternative Baseline Formulation:

Explore consistent formulations, i.e., modifications to VOF equation have consequence for momentum and energy transport; diffusive interface (DI); numerical signed-distance function

- Jain et al., “A conservative diffuse-interface method for compressible two-phase flows”, J. Comp. Phys. (2020)
- Jain, “Accurate conservative phase-field method for simulation of two-phase flows”, J. Comp. Phys. (2022)

$$+ \frac{\partial u_i f_j}{\partial x_j} \quad f_j = (\rho_L - \rho_G)(s_j + d_j)$$

Alternative CSF → local-CSF (l-CSF)

- Mirjalili et al., “Assessment of an energy-based surface tension model for simulation of two-phase flows using second-order phase field methods”, J. Comp. Phys. (2023)
- Cast to an “n”, “m”, “c” scheme, $c_M \sigma \kappa \alpha^n (1-\alpha)^m \nabla\alpha$; c = 1, n = m = 0 reverts to standard CSF

Diffuse interface method in an unstructured regime

- Hwang and Jain, “A phase-field method for simulations of two-phase flows on unstructured grids”, CTR Annual Briefs, 2022
- Local diffusion coefficient (local length and velocity) $d_j = C_\alpha |u_k - v_k| \epsilon \frac{\partial \alpha}{\partial x_j}$
- Full DI – only now in our incremental pressure projection scheme

Dam Break Validation: The Benefit of a Full Balanced-Force Method

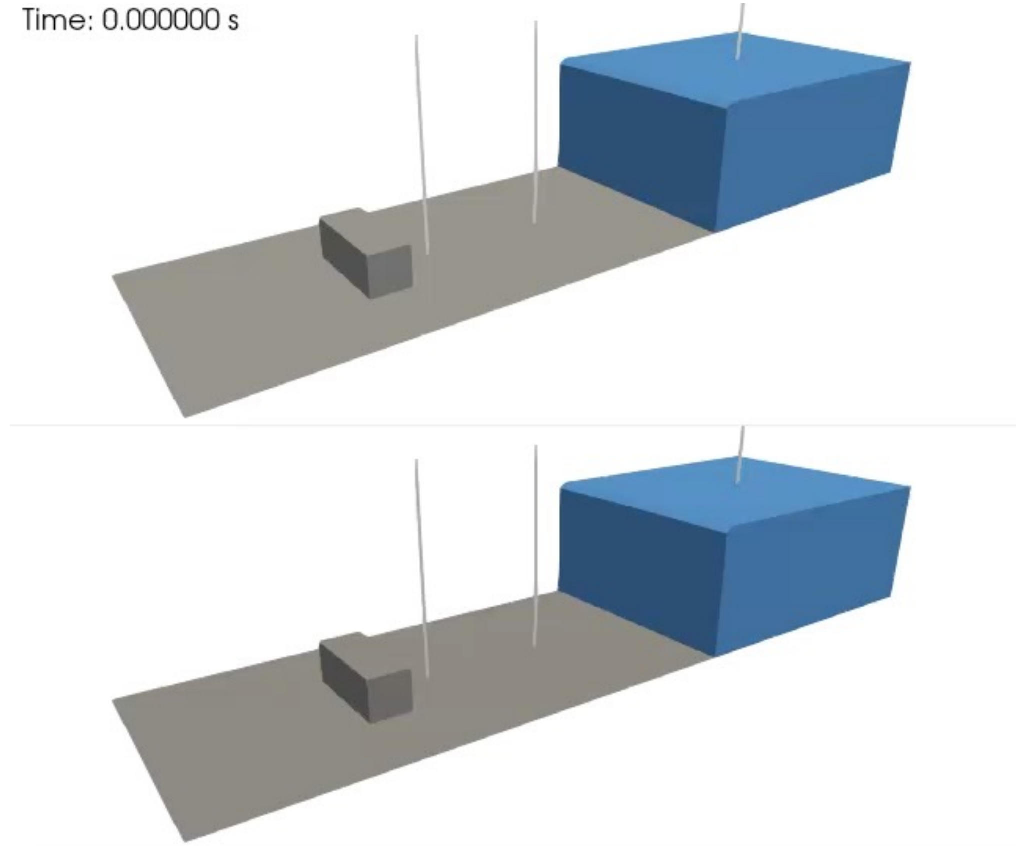

- Here, comparisons made between γ = 1 (top) and γ = 0 (bottom) showcasing the increased stabilizing effect of the set of all body forces in momentum included in the pressure stabilization formulation
- A nuance briefly captured and/or hinted at in seminal Francois et al., J. Comput. Phys. (2006) effort

$$\hat{u}_j = u_j^{R,k} - \Delta t \left(\frac{1}{\rho^*} \left(\frac{\partial p^k}{\partial x_j} - \sigma\kappa \frac{\partial \alpha}{\partial x_j} - \gamma \rho^* g_j \right) - \hat{G}_j p^k \right)$$

R0

Dam Break Validation: The Benefit of a Full Balanced-Force Method

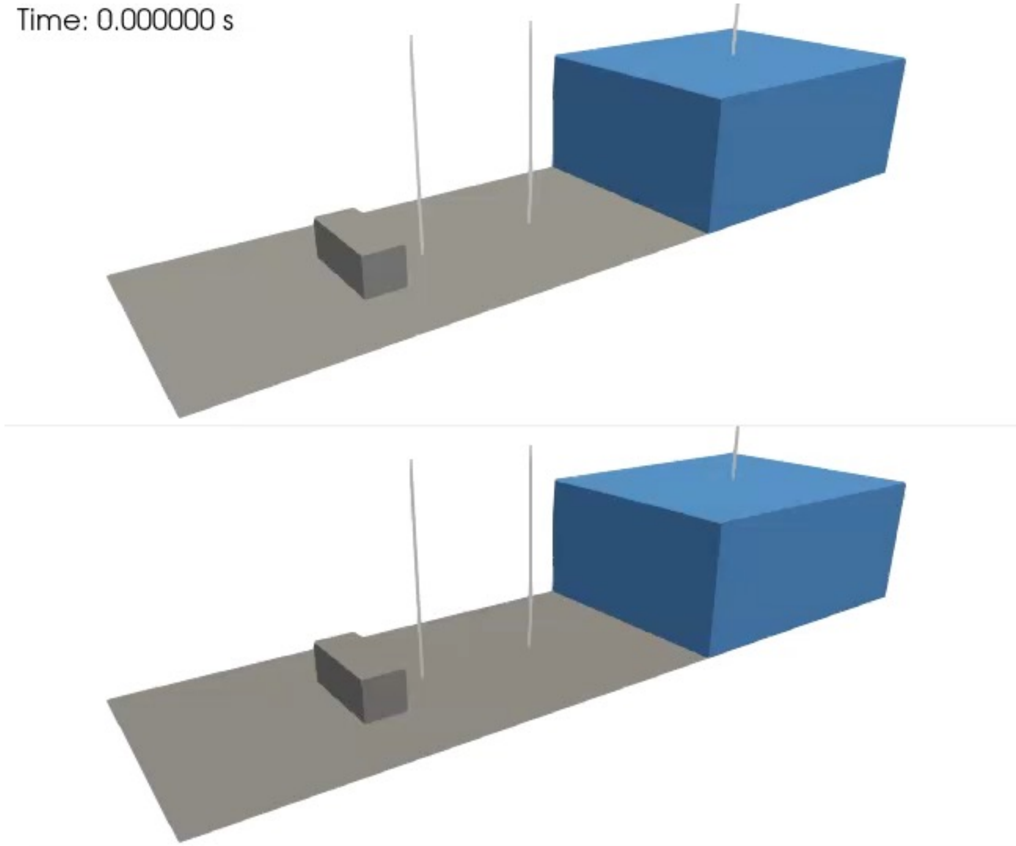

- Here, comparisons made between $\gamma = 1$ (top) and $\gamma = 0$ (bottom) showcasing the increased stabilizing effect of the set of all body forces in momentum included in the pressure stabilization formulation
- A nuance briefly captured and/or hinted at in seminal Francois et al., J. Comput. Phys. (2006) effort

$$\hat{u}_j = u_j^{R,k} - \Delta t \left(\frac{1}{\rho^*} \left(\frac{\partial p^k}{\partial x_j} - \sigma\kappa \frac{\partial \alpha}{\partial x_j} - \gamma \rho^* g_j \right) - \hat{G}_j p^k \right)$$

R2

Dam Break Validation

- Validation case of Kleefsman et al. "*A volume-of-fluid based simulation method for wave impact problems*", J. Comput. Phys. (2005).
- Qualitative comparisons also made to SNL's Sierra/Fuego, Brown et al. "*Modeling a rubble fire consisting of comingled liquid and solid fuel*", Tech. Rep. SAND2017-12318C (2017).

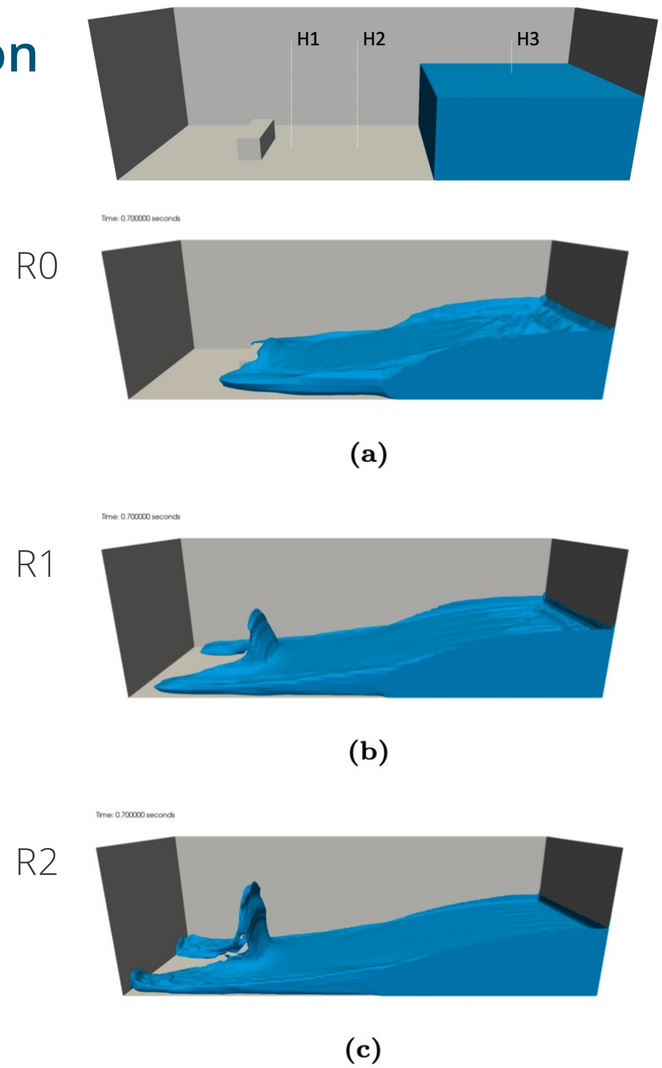

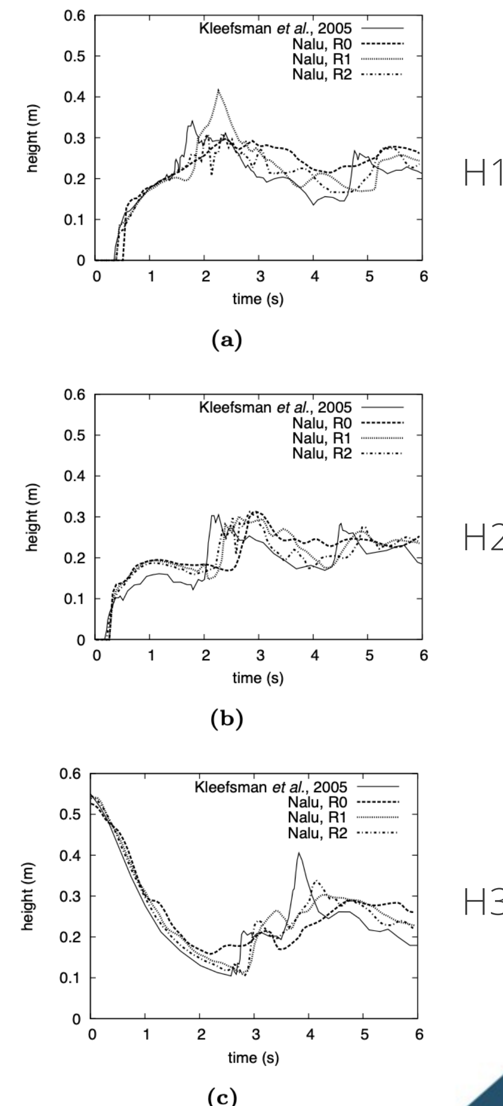

Overset: Freedom for Generalized Motion

- Implicit, constraint-based overset-based approach (DG/CVFEM-based, started)
- **Does not require presumed movement**
- Similar to Nalu-Wind’s Sharma et al, J. Comput. Phys. (2021), however, STK-based search

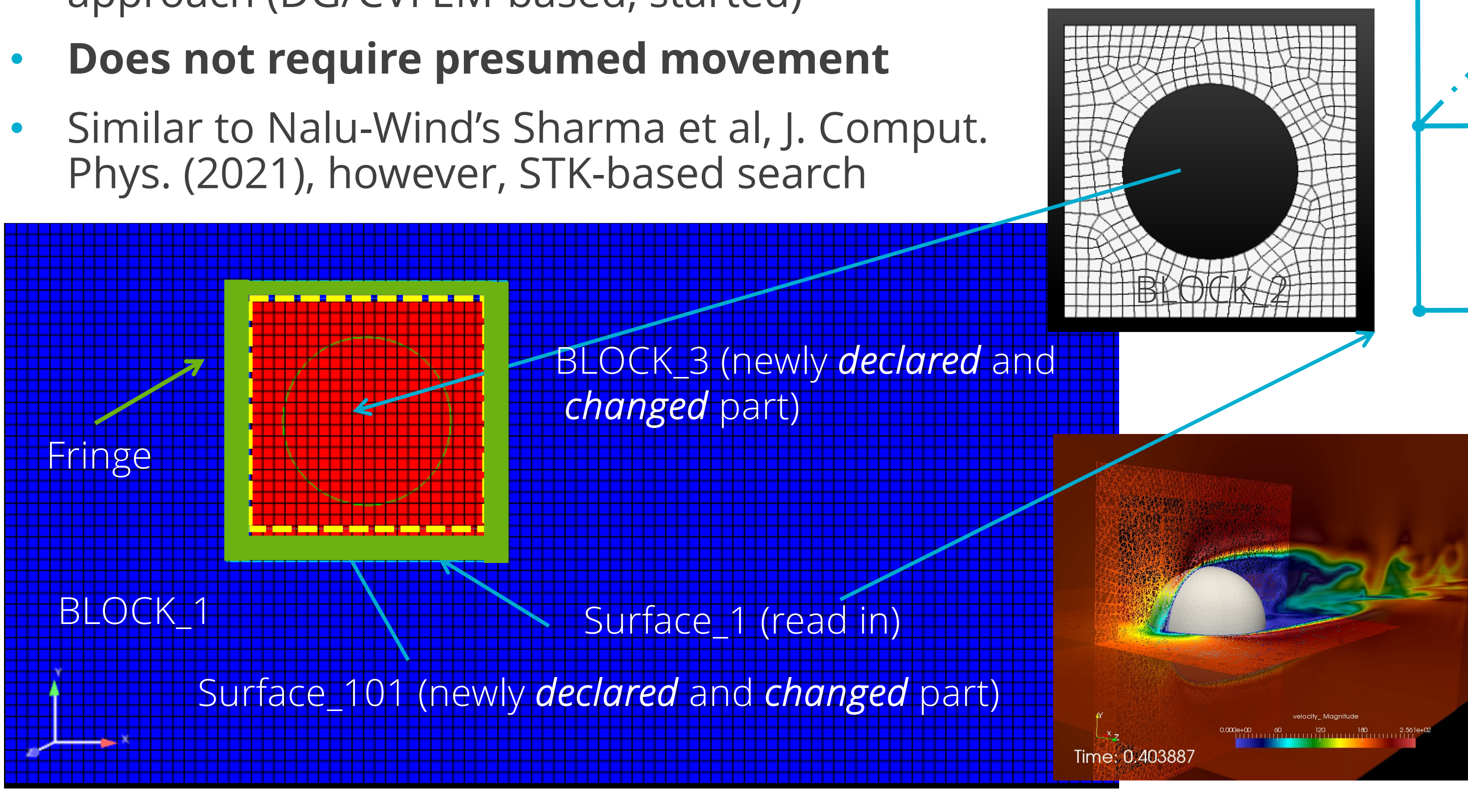

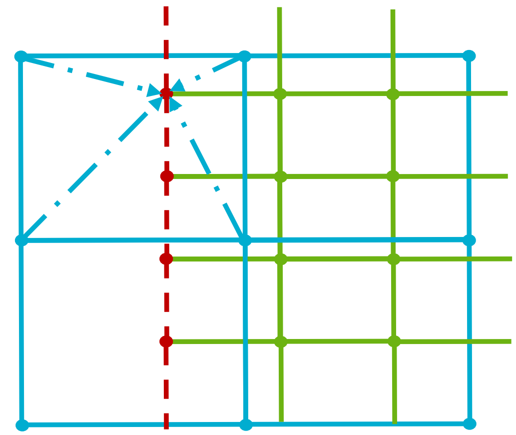

Constraint-based

Fluids Hex/Tet

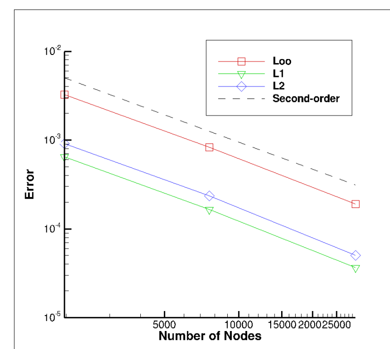

MMS

Objective: Overset + Volume of Fluid (VOF)

- Molenkamp verification case, now with overset
- Static bubble (computed curvature)

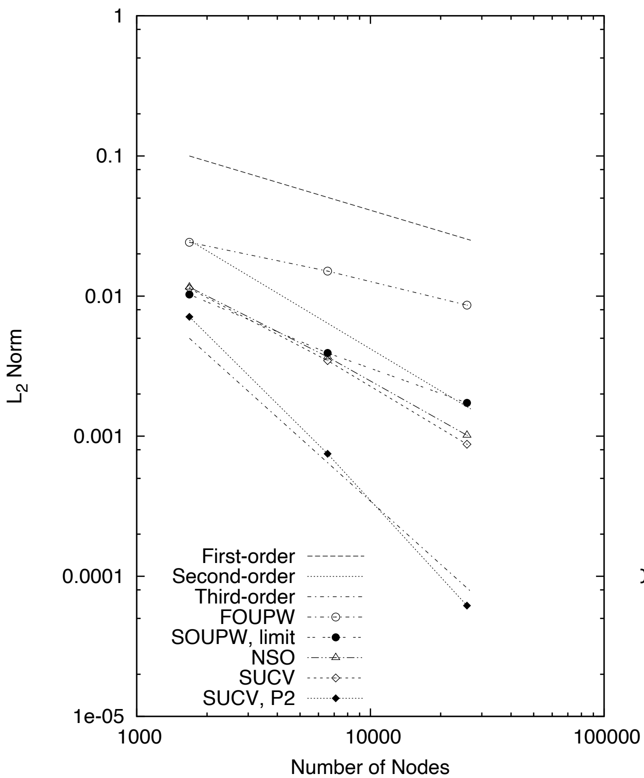

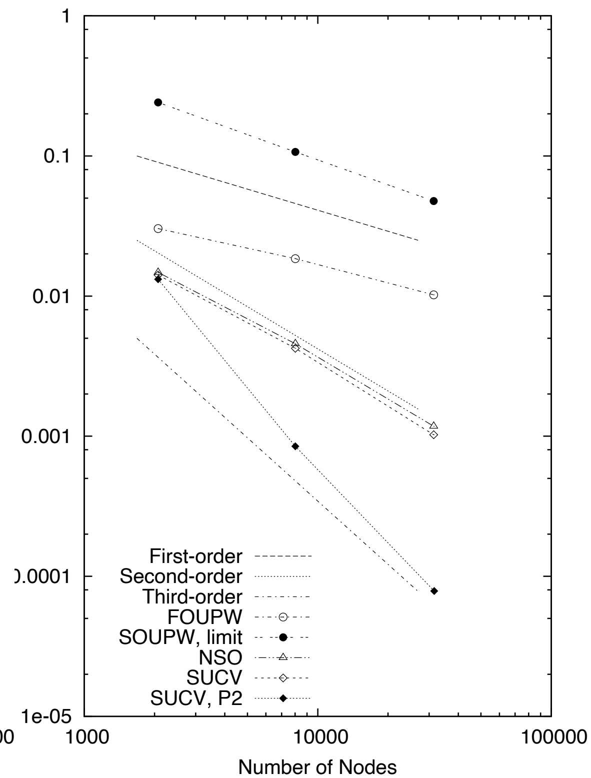

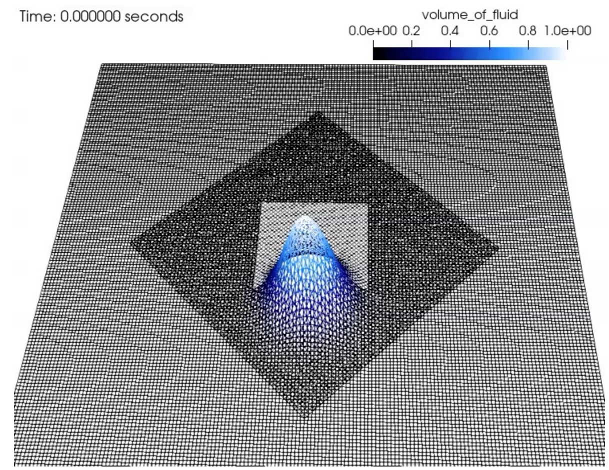

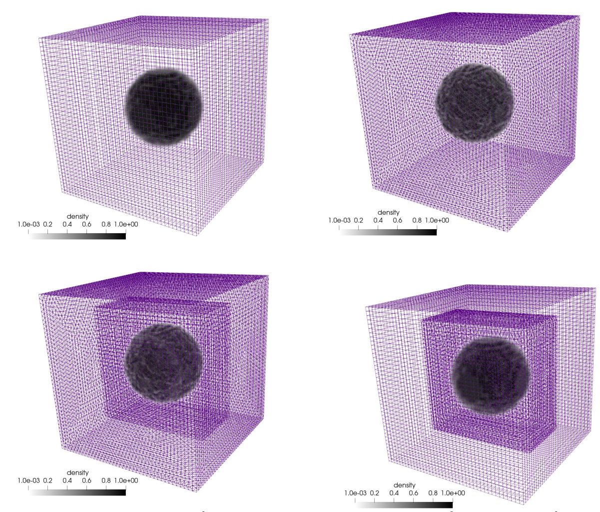

Hex8, Tet4, and Hex8/Tet4 Balanced Force static bubble; density ratio = 1000

Validation: Unmoored Buoy Drop (Quiescent Conditions)

- Comparisons are made to experimental data from the UK Centre for Marine Energy Research (UKCMER) of the WEC vertical displacement given in Ransley et al., Renew. Ener. (2017) who exercised a mesh deformation construct

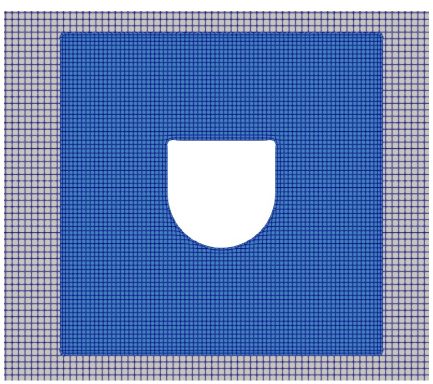

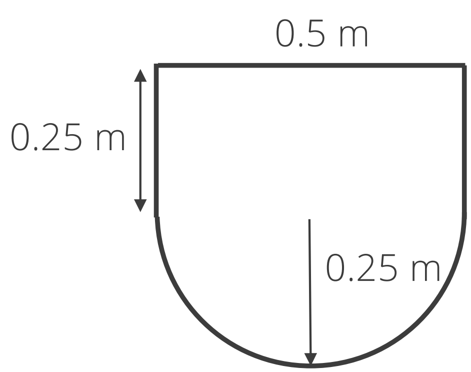

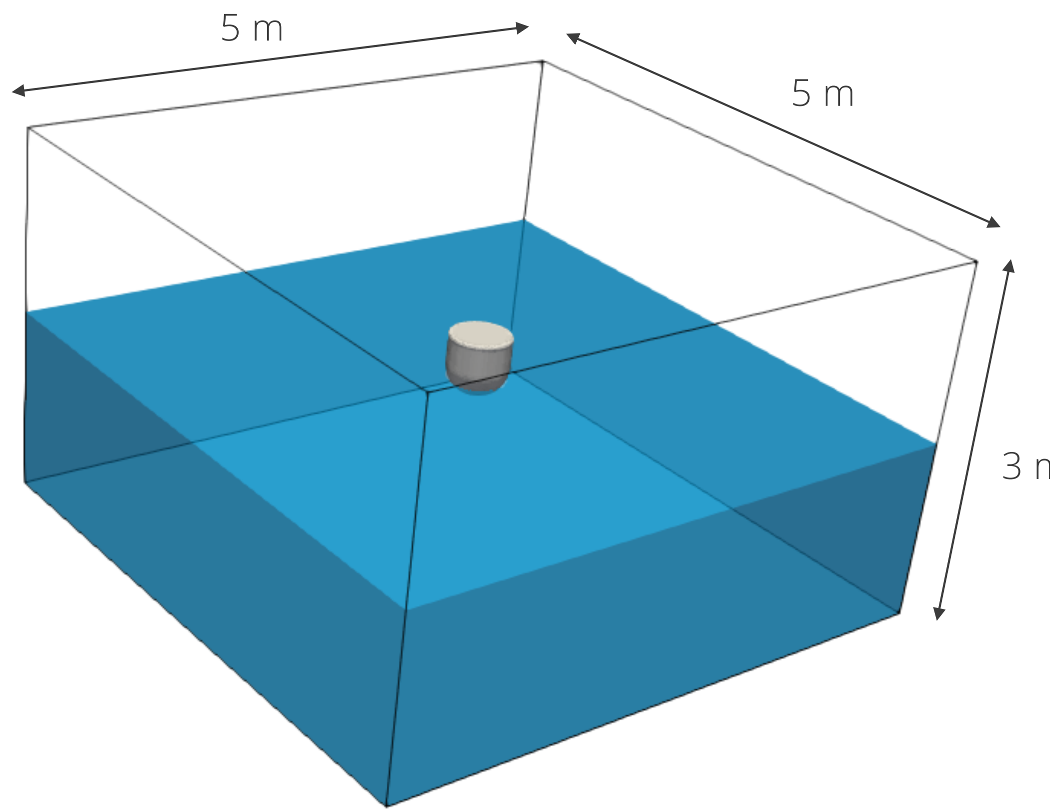

Validation: Unmoored Buoy Drop (Quiescent Conditions)

Objective: Compare to experimental dataset and demonstrate grid convergence

- Displaced buoy vertically; QoI: center of mass spatial location as a function of time

Finding: Improved comparison over other works found in literature, e.g., WEC vertical displacement given in Ransley et al., Renew. Ener. (2017)

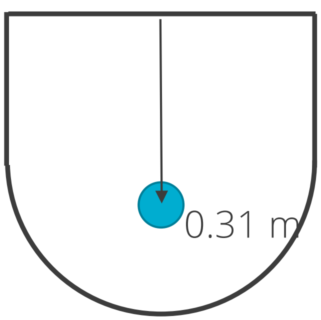

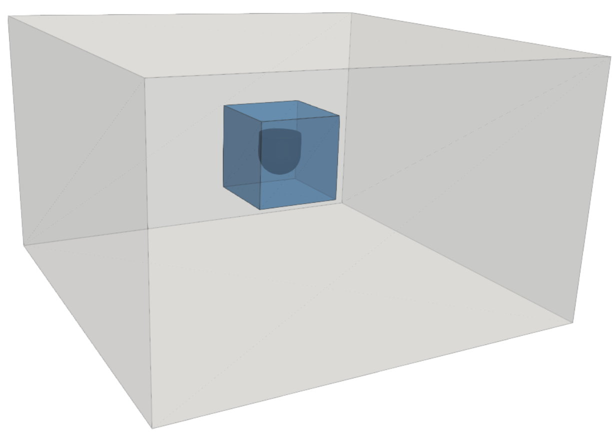

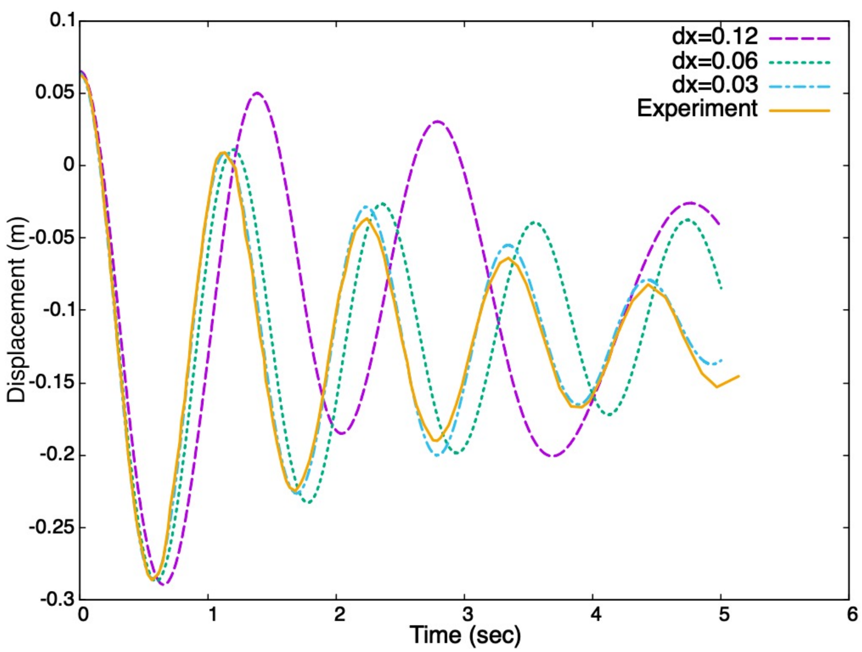

Validation: Moored Buoy Drop (Quiescent Conditions)

Objective: Compare to experimental dataset and demonstrate grid convergence – now tethered

- Displaced buoy vertically; QoI: center of mass spatial location as a function of time

Similar Finding: Improved comparison over other works found in literature, e.g., WEC vertical displacement given in Ransley et al., Renew. Ener. (2017)

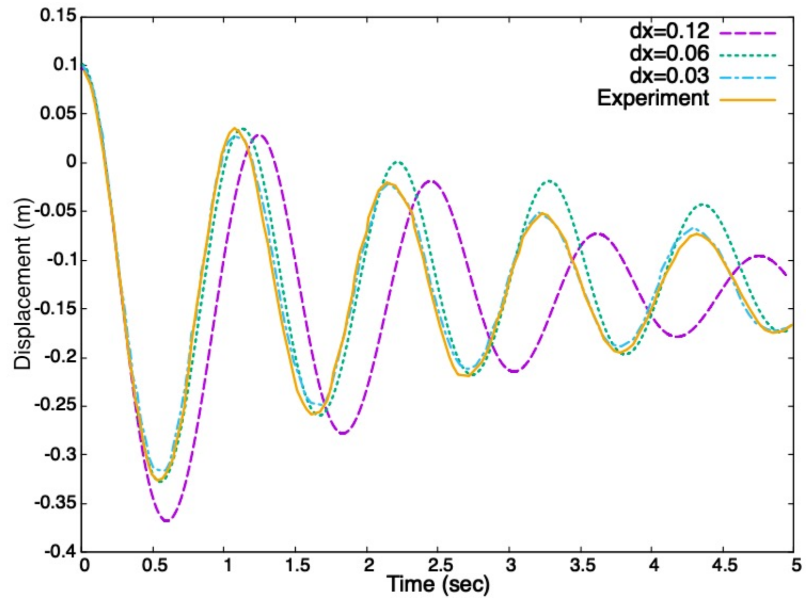

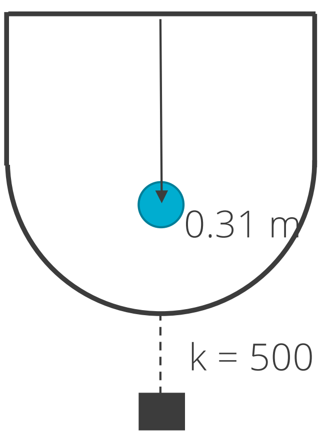

0.31 m

k = 500 N/m spring force

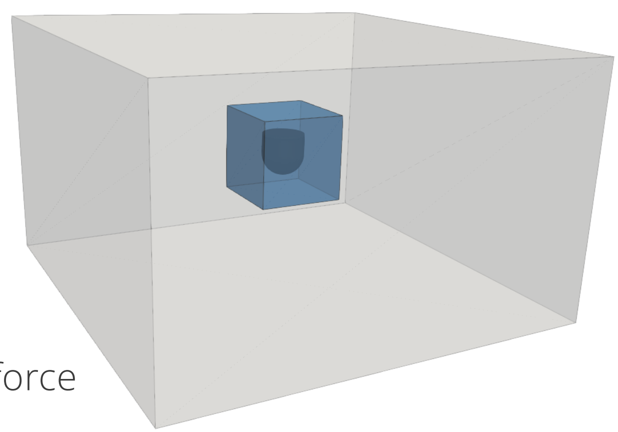

Buoy Dropped Into Quiescent Pool; large displacement limit Validation Benchmark, Domino and Horne, Renew. Energy (2022)

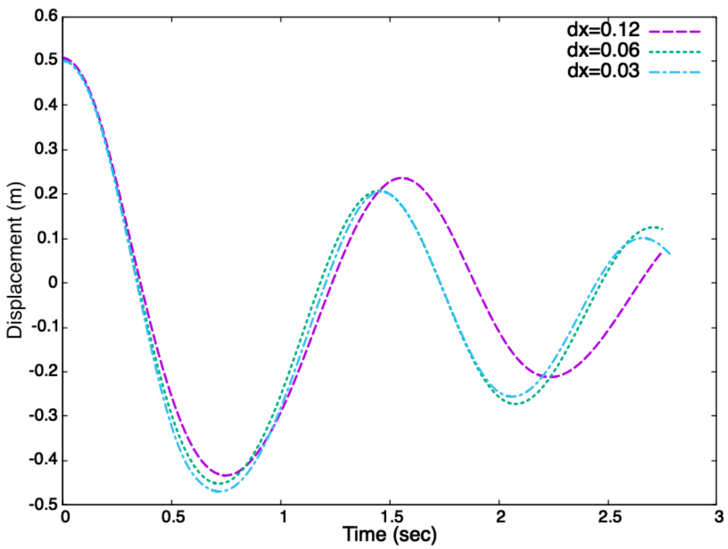

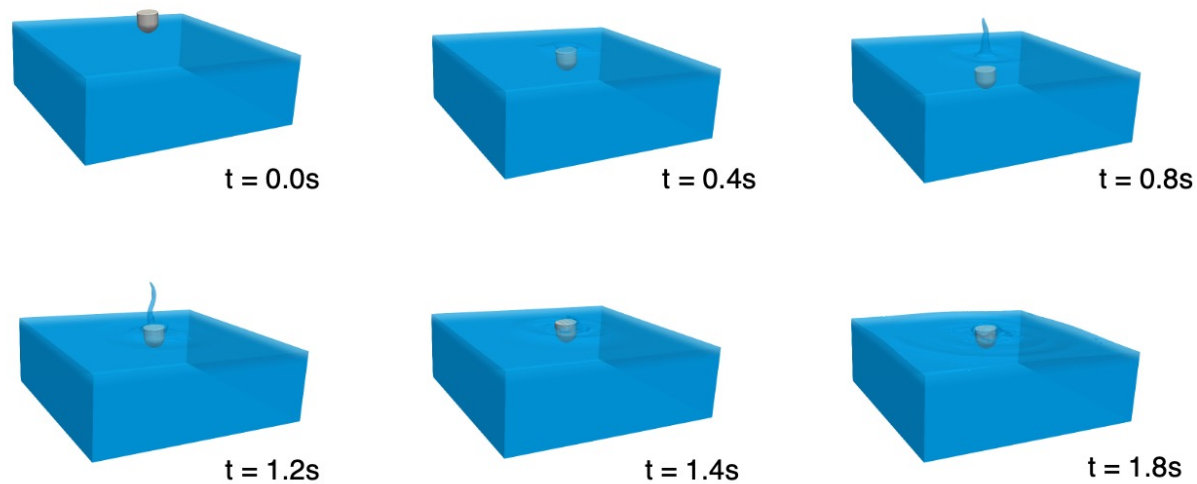

Large-displacement sample case run that can serve as a numerical benchmark

Buoy Subjected to large Wave-Form
Validation Benchmark, Domino and Horne, Renew. Energy (2022)

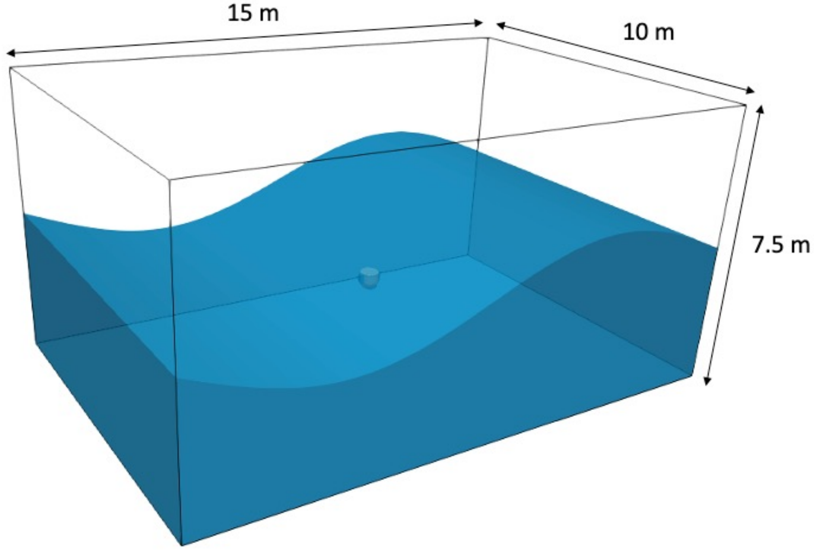

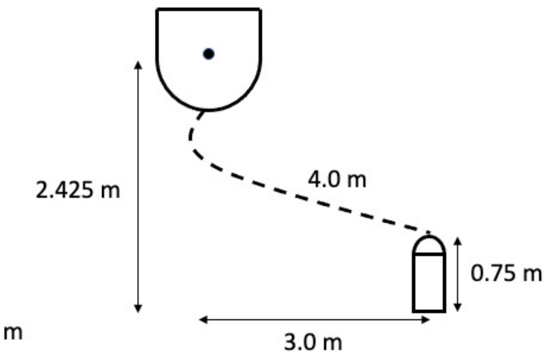

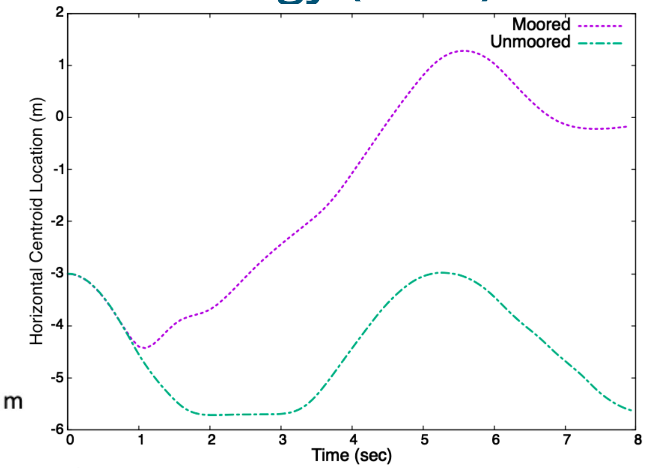

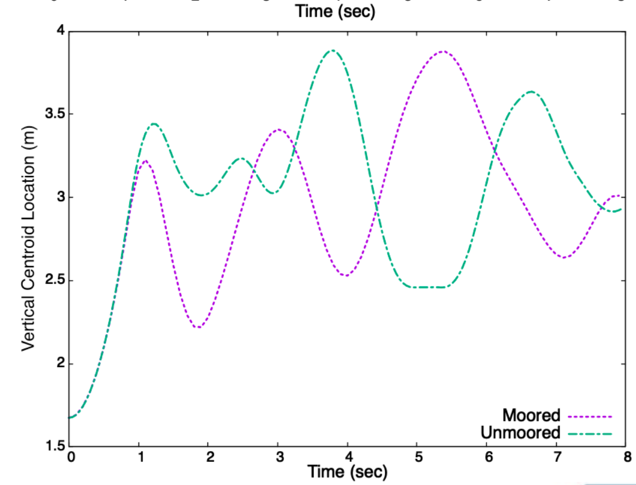

- Large-displacement sample case run that can serve as a numerical benchmark for the community; with and without mooring
- Geometric center = f(t) relative to the tether's mounting point

Buoy Subjected to large Wave-Form Validation Benchmark: Without (left) and With (right) Mooring

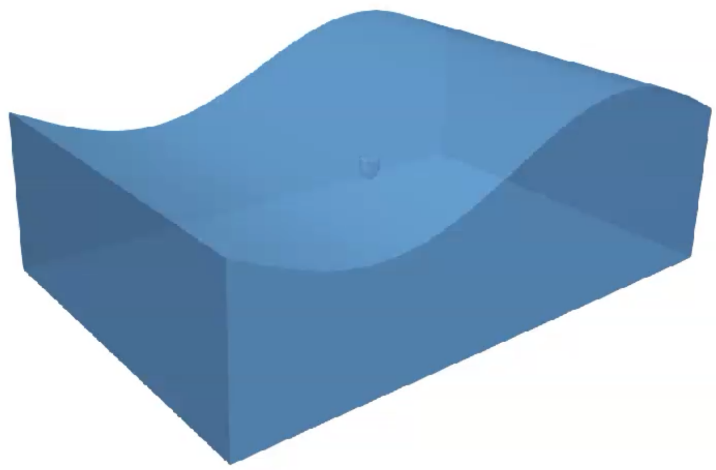

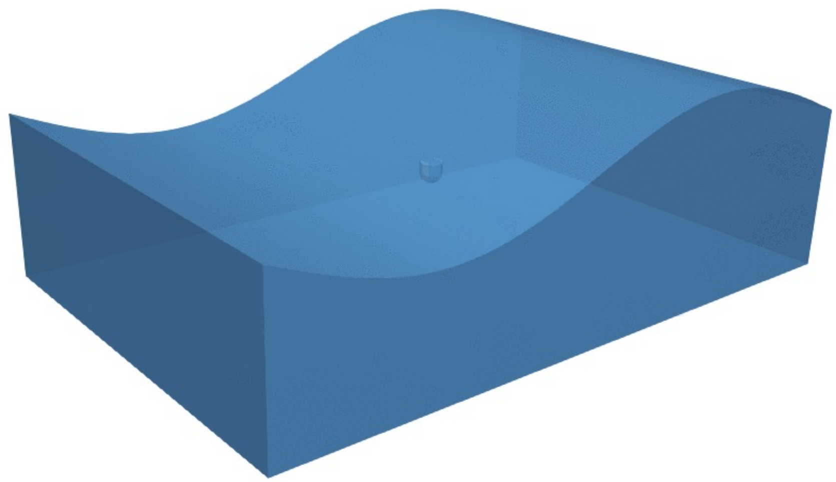

Re-visit Baseline Formulation: Capillary Instability Mitigation

Explore consistent formulations, i.e., modifications to VOF equation have consequence for momentum and energy transport; diffusive interface (DI); numerical signed-distance function

- Jain et al., "A conservative diffuse-interface method for compressible two-phase flows", J. Comp. Phys. (2020)
- Jain, "Accurate conservative phase-field method for simulation of two-phase flows", J. Comp. Phys. (2022)

Explore alternative CSF → local-CSF (l-CSF)

- Mirjalili et al., "Assessment of an energy-based surface tension model for simulation of two-phase flows using second-order phase field methods", J. Comp. Phys. (2023)
- Cast to an "n", "m", "c" scheme, $c_M \sigma \kappa \alpha^n (1-\alpha)^m \nabla\alpha$; c = 1, n = m = 0 reverts to standard CSF

Capillary Instabilities!!

- Denner et al., "Artificial viscosity model to mitigate numerical artefacts at fluid interfaces with surface tension", Comput. Fluids (2017):
  - $\Delta t < \sqrt{\frac{\rho_{ave} \Delta x^3}{2\pi\sigma}}$

Capillary Instabilities: Interface Evolution

Consistent Jain, J. Comp. Phys. (2022); *I-CSF* Mirjalili et al., J. Comp. Phys. (2023) noting:

- Explicit treatment of the surface tension momentum source term drives a stability limit due to operator-split volume of fluid field, and therefore, curvature (via CSF)
  - See many works, e.g., Denner et al, Comput. Fluids (2017)
- Consider Air/Water (σ = 0.07 N/m; g_y = -9.81 m/s^2) capillary instability configuration at 100 μm, mesh spacing of $5\text{x}10^{-7}$ m
  - Stability limit $\Delta t \sim 1.0\text{x}10^{-8}$ s; initial condition (far left)

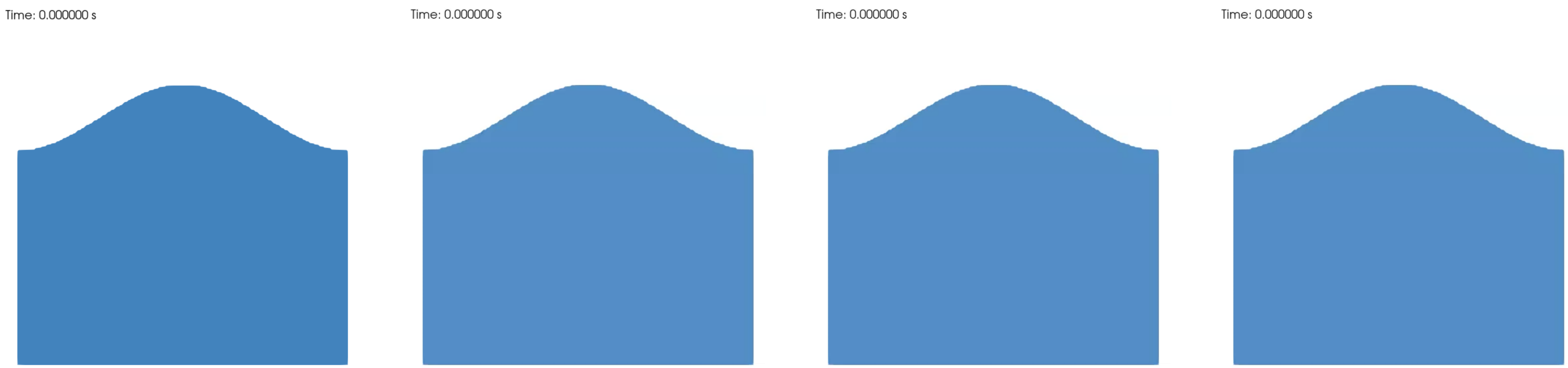

100 μm | $\Delta t = 1\text{x}10^{-6}$ s | $\Delta t = 1\text{x}10^{-7}$ s | $\Delta t = 1\text{x}10^{-8}$ s

Capillary Instabilities: Interface Evolution

- Post-processed centerline interface height as a function of time
- Note that many capillary instability works follow: Popinet, “An accurate adaptive solver for surface-tension-driven interfacial flows”. J Com. Phys. (2009) where density ratio is unity, with varying viscosity and surface tensions, and very small initial amplitude
- I will showcase the like-density case a bit later

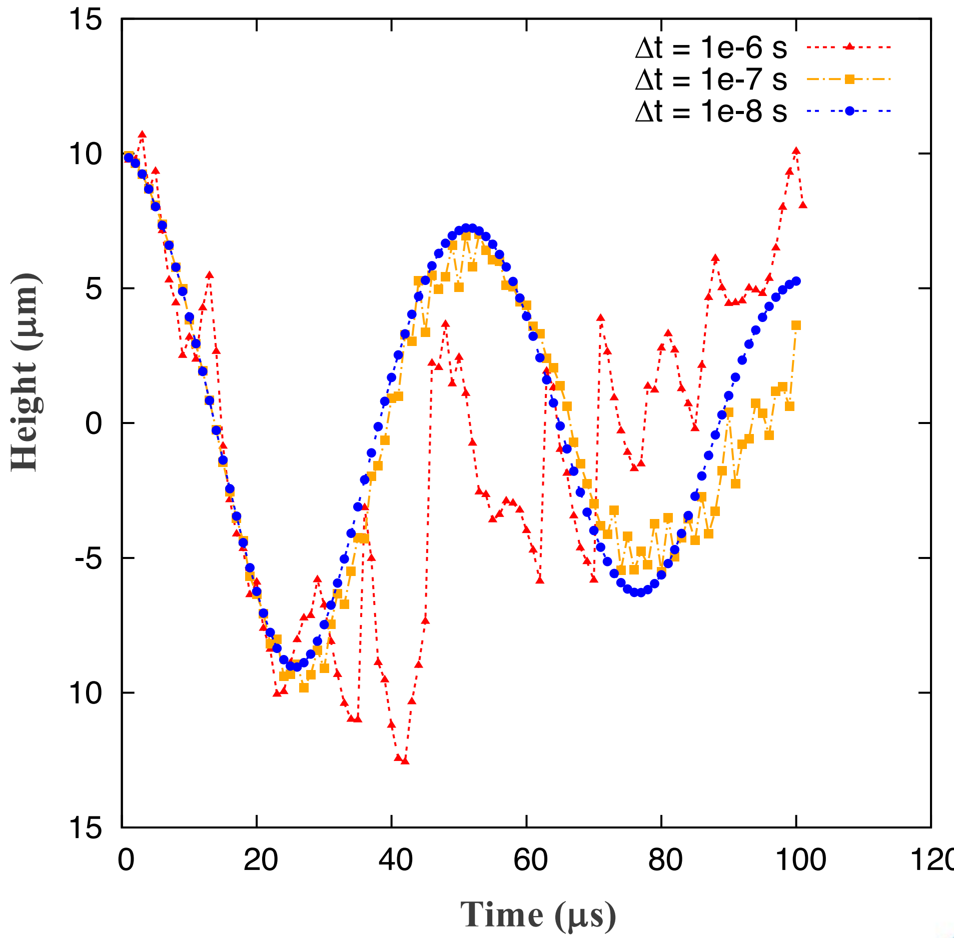

Capillary Instabilities: Path Forward

- Denner et al., “Artificial viscosity model to mitigate numerical artefacts at fluid interfaces with surface tension”, Comput. Fluids (2017) outlines a baseline model of,
  - Raessi et al. “A semi-implicit finite volume implementation of the CSF method for treating surface tension in interfacial flows”, Int. J. Numer. Methods Fluids (2009), where an artificial viscosity is provided, $F_i^{\sigma} = \sigma \Delta t |\nabla \alpha| \nabla_s^2 u_i$; ∇_s^2 is the Laplace-Beltrami operator tangential to the interface
  - Follows the Hysing, “A new implicit surface tension implementation for interfacial flows”, Int. J. Numer. Methods Fluids (2006)
  - Hysing (2006) implementation, that has it’s roots to a Sandia ***Goma*** effort, see: Cairncross et al., “A finite element method for free surface flows of incompressible fluids in three dimensions. Part I. Boundary fitted mesh motion”, Int. J. Num. Methods Fluids (2000)
  - This operator can be interpreted as an artificial tangential shear stress that damps out instabilities
- Monolithic schemes are also postulated where additional DOFs include interface normal and curvature, allowing 100x increase in time steps over the stability limit, see: Denner et al., “Breaching the capillary time-step constraint using a coupled VOF method with implicit surface tension”, J. Comput. Phys. (2022)
  - This scheme could be implemented within Sandia’s arbitrary coupling/monolithic codes (Sierra/Aria) without too much trouble, however, we would like to avoid fully implicit, monolithic systems including momentum, continuity, VOF, surface normal, and curvature

Capillary Instabilities: Denner et al. (2017) Stabilization

How does this stabilization approach perform?

- Looks like we bought a factor of 10 in time step, while the $1\text{x}10^{-8}$ results look nearly identical to the non-stabilized scheme

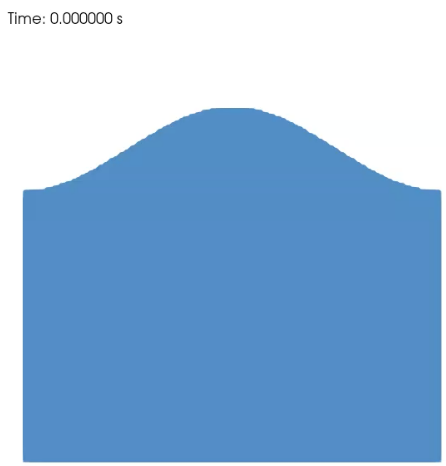

$\Delta t = 1\text{x}10^{-6}$ s

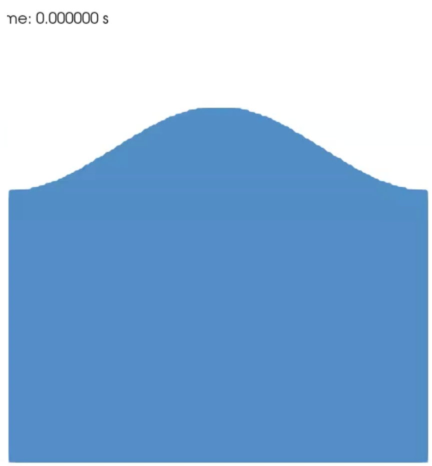

$\Delta t = 1\text{x}10^{-7}$ s

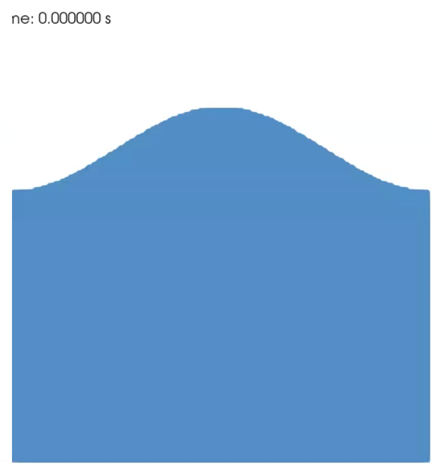

$\Delta t = 1\text{x}10^{-8}$ s

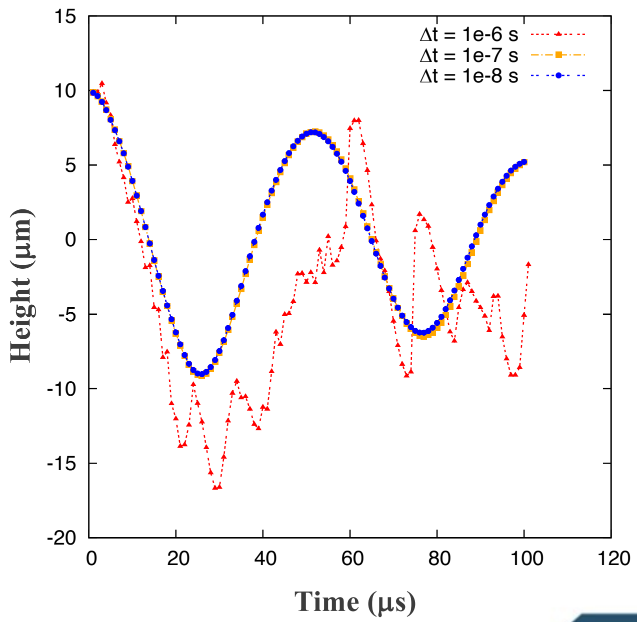

Comparison to Analytical Solution: Verification

- Following: Popinet, J Comp. Phys. (2009) as presented by Nobel et al., "A Conformal Decomposition Finite Element Method for Dynamic Wetting Applications", FEDSM2017;
  - Ohnesorge number *Oh* = μ /(σ ρ λ)1/2 = 1/√3000
  - Dimensionless viscosity ε = μ κ 2 /(ρ ω_0) = 6.47×10^{-2}
  - ω_0 = 1; like density and viscosity between the phases
- For this configuration (domain unity in height and width), the time step taken was ~25x higher than the stability limit (including capillary stabilization)

Use this case to explore alternatives to curvature calculations, Jain, J. Comput. Phys. (2022) and inclusion of a diffuse interface approach

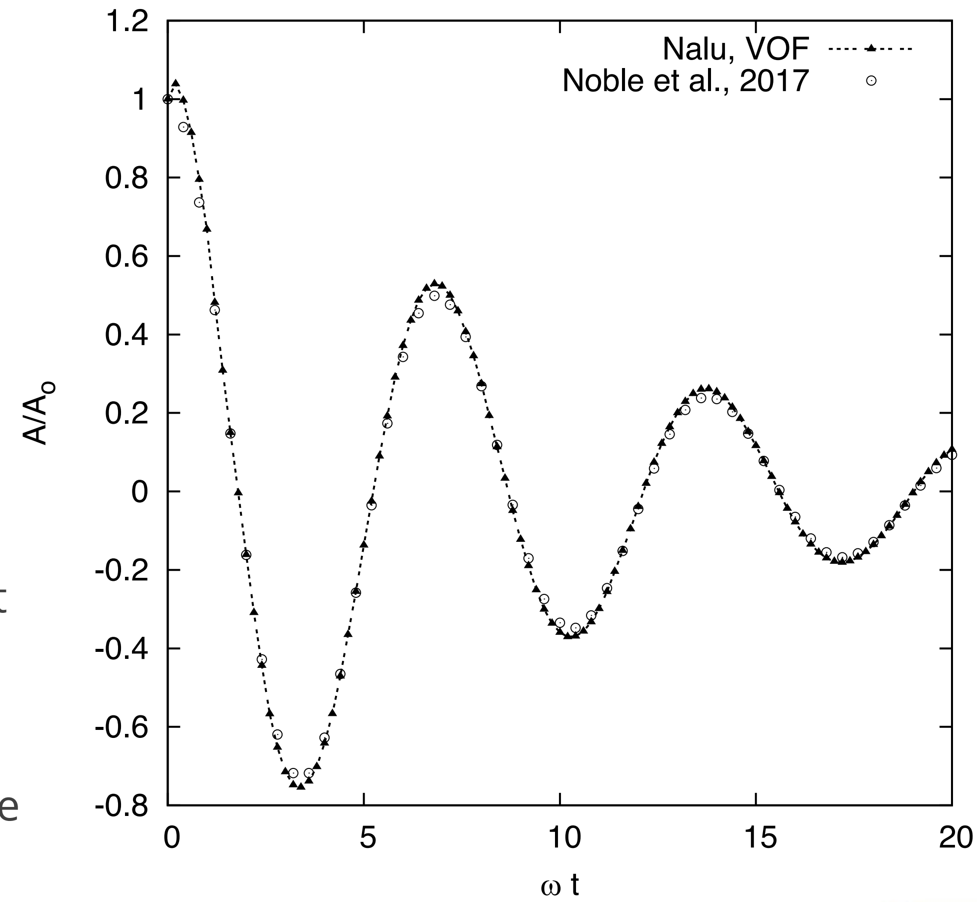

Realistic Flows of Ishikawa et al. Chem. Engr. Process (2022)

- Ishikawa et al., “Numerical study on mass transfer in a falling film on structured plates with micro-baffles”, Chem. Engr. Process (2022) motivated falling film simulation result (a) at 0.035 seconds depicting the 90º (b) and 45º (c) unrotated configuration (image scaled in x-direction) 0.1 mm (100 μm) baffle heights
- Capillary stabilization activated; localized CSF, consistent momentum source term
  - The time step roughly 13 times the stability limit

Now stable at the 100 μm scale!

(b)

(c)

(a)

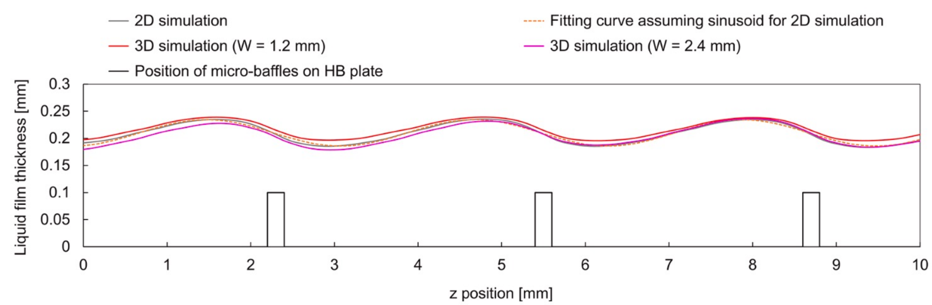

Fig. 7. 2D- and 3D-simulated gas-liquid interface location for the HB plate (Case 2D-1, Case HB-6, and Case HB-15 in Table A1).